HHS Public Access

Author manuscript

Obesity (Silver Spring). Author manuscript; available in PMC 2016 February 01.

Published in final edited form as:

Obesity (Silver Spring). 2015 February ; 23(2): 399–407. doi:10.1002/oby.20971.

Adipose tissue remodeling in a novel domestic porcine model of diet-induced obesity

Aditya S. Pawar[1,*], **Xiang-Yang Zhu**[1,*], **Alfonso Eirin**[1], **Hui Tang**[1], **Kyra L. Jordan**[1], **John R. Woollard**[1], **Amir Lerman**[2], and **Lilach O. Lerman**[1,2]

[1]The Division of Nephrology and Hypertension, Mayo Clinic, Rochester, MN 55905

[2]The Division of Cardiovascular Diseases, Mayo Clinic, Rochester, MN 55905

Abstract

Objective—To establish and characterize a novel domestic porcine model of obesity.

Design and Methods—Fourteen domestic pigs were fed normal (lean, n=7) or high-fat/high-fructose diet (obese, n=7) for 16 weeks. Subcutaneous abdominal adipose tissue biopsies were obtained after 8, 12 and 16 weeks of diet, and pericardial adipose tissue after 16 weeks, for assessments of adipocyte size, fibrosis, and inflammation. Adipose tissue volume and cardiac function were studied with multi-detector computed-tomography, and oxygenation with magnetic resonance imaging. Plasma lipids profiles, insulin resistance, and markers of inflammation were evaluated.

Results—Compared with lean, obese pigs had elevated cholesterol and triglycerides levels, blood pressure, and insulin resistance. Both abdominal and pericardial fat volume increased after 16 weeks of obese. In abdominal subcutaneous adipose tissue, adipocyte size and both tumor necrosis factor (TNF)-α expression progressively increased. Macrophage infiltration showed in both abdominal and pericardial adipose tissues. Circulating TNF-α increased in obese only at 16 weeks. Compared with Lean, obese pigs had similar global cardiac function, but myocardial perfusion and oxygenation were significantly impaired.

Conclusion—A high-fat/high-fructose diet induces in domestic pigs many characteristics of metabolic syndrome, which is useful to investigate the effects of the obesity.

Keywords

Obesity; insulin resistance; fat metabolism; inflammation

Correspondence: Lilach O. Lerman, MD, PhD, Division of Nephrology and Hypertension, Mayo Clinic, 200 First Street SW, Rochester, MN, 55905. Lerman.Lilach@Mayo.Edu, Phone: (507)-266-9376. Fax: (507)-266-931.

*The two authors contributed equally to the manuscript

Disclosure of potential conflicts of interest

None

Introduction

Obesity has become an important clinical and public health burden worldwide. Its prevalence is on a rampant increase, leading to increased morbidity and mortality due to cardiovascular (CV) disease[1]. The metabolic syndrome doubles the risk for CV disease, more than triples the risk for CV mortality, and raises the risk for diabetes about 5 fold[2]. Visceral obesity is a major component of metabolic syndrome.[3, 4] Subsequent development of insulin resistance, which characterizes metabolic syndrome, is associated with microvascular (MV) dysfunction, and aggravates myocardial inflammation, oxidative stress, and fibrosis[5].

An important factor linking metabolic syndrome and development of CV disease is the activity of the adipose tissue, an endocrine organ that secrets humoral factors (adipokines) and pro-inflammatory cytokines, causing a chronic low-grade inflammation and insulin resistance. In particular, macrophages have been implicated in adipose inflammation and systemic metabolic abnormalities[6]. Adipose tissue inflammation contributes to the emergence of many pathological features that characterize the metabolic syndrome and result in atherosclerosis and CV disease[7].

The pericardial adipose tissue might be particularly perilous for the heart, because of its anatomic proximity to the myocardium. Correlations between increased epicardial adipose tissue and impaired cardiac dysfunction led to the postulation that epicardial adipose tissue may release inflammatory cytokines to the vascular wall, impairing coronary vascular function[8, 9].

However, elucidation of pathological mechanisms underlying the CV risk in metabolic syndrome is hampered by the limited availability of pre-clinical animal models of metabolic syndrome. We have previously shown that domestic farm pigs fed 2% high cholesterol diet develop endothelial dysfunction and early changes of atherosclerosis in blood vessels, heart and kidney,[5, 10-12] but not insulin resistance or hypertension. A high fat and fructose diet can induce insulin resistance in rats[13, 14] and Ossabaw mini-pigs[15, 16], but whether it can induce the Metabolic syndrome in domestic pigs has not been fully clarified. This study was designed to develop and characterize the evolution of metabolic syndrome in a domestic pig model. We tested the hypothesis that domestic pigs fed with high fat/fructose diet would develop obesity with insulin resistance, which would be associated with pathological fat remodeling.

Method

1. Study protocols

The Institutional Animal Care and Use Committee approved this study. Fourteen 3-months old female domestic pigs were randomized in two groups (n=7 each): Control (Lean) pigs were fed standard chow (13% protein, 2% fat, 6% fiber, Purina Animal Nutrition LLC, MN), and obese with a high-fat/high-fructose diet fed ad libitum (5B4L, protein 16.1%, ether extract fat 43.0%, and carbohydrates 40.8%, Purina Test Diet, Richmond, Indiana), for a total of 16 weeks, with free access to water. At 8, 12, and 16 weeks, subcutaneous

abdominal adipose tissue biopsies and fasting blood samples were collected under anesthesia and sterile conditions in all pigs. At 16 weeks, the pigs were studied in-vivo with magnetic resonance imaging (MRI, for myocardial oxygenation) followed by multi-detector computed-tomography (MDCT, for cardiac structure, function, and myocardial perfusion) 2 days later. Three days following the completion of *in-vivo* studies, pigs were euthanized with pentobesearbital-sodium (100mg/kg IV, Sleepaway®, Fort Dodge Laboratories, Fort Dodge, Iowa). Terminal pericardial and subcutaneous abdominal adipose tissue biopsies were collected and tissue studies performed for assessments of fat inflammation and remodeling.

2. Systemic measurements

Arterial blood pressure was directly measured through a catheter inserted in the right carotid artery using a pressure transducer before MDCT scanning. Heart rate was monitored and recorded during MRI and MDCT studies. Rate pressure products (heart rate × systolic blood pressure) were calculated as an index of oxygen consumption. Systemic levels of monocyte chemoattractant protein (MCP)-1 and tumor necrosis factor (TNF)-alpha (Invitrogen Life Technology, Grand Island, NY) were tested by ELISA, as previously described[17], and total cholesterol, triglycerides, low-density lipoproteins (LDL), and high-density lipoprotein (HDL) by standard procedures. Intravenous glucose tolerance test (IVGTT) was performed at 12 and 16 weeks and the homeostasis-model-assessment of insulin resistance (HOMA-IR) (fasting plasma glucose ×fasting plasma insulin/22.5) used as an index of insulin resistance[5].

2. In Vivo Studies

Each *in vivo* study constituted of MRI followed by MDCT studies 2 days apart. For each study animals were weighed, induced with IM Telazol (5mg/kg) and xylazine (2 mg/kg), intubated, and ventilated with room air.

MRI—Blood Oxygen Level-Dependent (BOLD)-MRI was performed to evaluate myocardial oxygenation[18-22]. Briefly, under 1-2% isoflurane anesthesia, pigs were positioned in the MRI scanner (Signa Twin Speed EXCITE 3T system, GE Healthcare, Waukeshau, WI) and BOLD images (4-5 axial-obeselique) acquired along the cardiac short axis during suspended respiration. Gated Spoiled Gradient Echo (SPGR) sequence with TR/TE/number of echoes/Matrix size/FOV/Slice thickness/Flip cardiac angle = 20.5 ms/2 ms/8/128x128/35/0.5 cm/30°. Imaging was repeated during intravenous injection of adenosine (400 μg/kg/min) through an ear vein catheter. BOLD data was processed in MATLAB 7.10 (The MathWorks Inc., Natick, MA). The BOLD index, R_2*, was estimated in each voxel by fitting the MR signal intensity vs. echo time to a single exponential function and calculating the MR intensity decay rate. Myocardial R_2* values were estimated from regions of interest (ROI) defined based on T_2*-weighted MR images and calculating R_2* weighted-average of all ROIs.

MDCT—MDCT scanning (Somatom Sensation-64, Siemens Medical Solution, Forchheim, Germany) was performed 2 days after MRI to evaluate cardiac structure and function as described[23] including cardiac systolic, diastolic, and vascular endothelial function. Briefly, mid left ventricle (LV) levels were selected for evaluation of microvascular perfusion and

function. A bolus injection of nonionic, low-osmolar contrast medium (iopamidol-370, 0.33 ml/kg over 2 s) into the right atrium was immediately followed by a 50-s flow study during respiratory suspension at end expiration. Fifteen minutes later, the functional study was repeated during a 5-min intravenous infusion of adenosine (400 μg/kg/min). Two parallel 6-mm-thick cardiac sections were investigated throughout the cardiac cycle with a full-scan reconstruction (330 ms) at 50-ms increments. The entire LV was also scanned 20 times throughout the cardiac cycle to obtain multilevel images for cardiac systolic and diastolic functions[23, 24].

CT data analysis

Cardiac measurement: All Images were analyzed with the Analyze™ software package (Biomedical Imaging Resource, Mayo Clinic, Rochester, MN), as we have reported previously[23, 24]. For LV function, the LV endocardial surfaces were traced at end diastole and systole. Stroke volume, cardiac output, and LV ejection fraction were calculated as shown previously[23, 24] Early (E) and late (A) LV filling rates were calculated from the positive slopes of the LV volume/time curve[25]. Myocardial perfusion was calculated from time-density curves generated secondary to transit of contrast media[26].

Fat volume measurement: Subcutaneous adipose tissue was traced in 15 abdominal slides from the middle level of kidney on MDCT image analysis and expressed as volume and fraction, modified from previously descripted[5, 10, 19, 27]. For pericardial fat volume, a ROI was traced surrounding the heart on the MDCT-derived cross-sections throughout its entire volume, and pericardial fat then measured based on the attenuation range for fat, and expressed as ratio to the volume of the heart[5, 27].

4. Exvivo Studies

RT-PCR—Frozen abdominal or pericardial fat tissues (~50mg) were homogenized in 350ul of ice cold lysis buffer, supplied by mirVana PARIS total RNA isolation kit (Life Technologies, Cat# AM1556).

Total RNA was then isolated from homogenized samples, and its concentration measured by a Spectrophotometer (NanoDrop). 50μl of the RNA samples were then treated with 2 units for rDNase (Life Technologies, Cat# AM1906) to remove possible contaminating DNA. First-strand cDNA was produced from 300ng of total RNA using SuperScript VILO cDNA Synthesis kit (Life Technologies, Cat#11754-050). Relative quantitative PCR was performed using Taqman assays, containing 20ng of cDNA products. Taqman assays included the followings: iNOS (Ss03374608), CD86 (Ss03394398), mannose-receptor (Ss03373693), CD11c (AJ1RVEU), TNF-a (Ss03391318), IL-6 (Ss03384604), CD-68 (AJWR2PY), arginase-1 (Ss03391398) and GAPDH (Ss03374854, for internal control), all from Life Technologies. Negative controls with no cDNA were cycled in parallel with each run. PCR analysis was done on Applied Biosystems ViiA7 Real-Time PCR systems at the following conditions: 50°C for 2 minutes, 95°C for 10 minutes and 40 cycles of 95°C for 15 seconds and 60°C for 1 minute. Fold-changes of each target gene in the obese relative to lean group were calculated using the $2^{-\Delta\Delta CT}$ method. Fold changes greater than 2 are considered as significant.

Histology—Adipose tissue fibrosis was analyzed on trichrome stained slides and capillaries manually counted under high power field of microscope (100x). Immunohistochemistry was performed in 5 μm of either frozen or paraffin-preserved sub-cutaneous and pericardial adipose tissue following standard protocols. Inflammation was assessed by TNF-alpha (abcam 1:50), IL-6 (1:50, Abcam), monocyte chemotactic protein-1 (MCP-1), macrophage staining (CD68, abcam 1:50) and their subpopulations, inducible nitric oxide synthase (iNOS) for pro-inflammatory M1-phenotype, and arginase-1 for reparative M2-phenotype (both Abcam 1:50). Image analysis utilized a computer-aided image-analysis program (AxioVision® Carl Zeiss Micro Imaging, Thornwood, NY). Fibrosis results were expressed as percent of trichrome staining per field. Capillary numbers were expressed per field and all immunohistochemistry results as positive area/total cellular nuclei area. M1 macrophages were quantified as CD68/iNOS double positive area/total cellular nuclei area, and M2 macrophages as CD68/Arginase-1 double positive area/total cellular nuclei area.

5. Statistical Analysis

Statistical analysis was performed using JMP software package version 8.0 (SAS Institute, Cary, NC). Results were expressed as mean±SEM for normally distributed data. Comparisons within groups were performed using paired Student's t-test and among groups using ANOVA or Wilcoxon when appropriate. $p \leq 0.05$ was considered statistically significant.

Results

Systemic characteristics

All animals had similar body weight at baseline, but obese pigs gained weight faster than lean (Figure 1A). Fasting HOMA-IR levels were significantly increased in obese at 16 weeks (Table 1). IVGTT results showed that at all time points plasma insulin levels were increased in obese compared to lean pigs at both 12 and 16 weeks, while glucose levels were increased only at early time point (Figure 1B and C). In obese pigs, total cholesterol, LDL, HDL, and serum triglycerides were elevated at 12 and 16 weeks. In lean pigs, both total cholesterol and triglycerides fell at 16 compared with 12 weeks, while in obese only triglycerides fell, but remained higher than in lean pigs (Figure 1D and E). Plasma adiponectin levels were similar between lean and obese pigs at both 12 and 16 weeks, but fell only in obese pigs at 16 compared with 12 weeks (Figure 1F). By 16 weeks mean arterial pressure was elevated in obese pigs compared with lean (Table 1). Circulating MCP-1 and TNF-α level were both significantly increased (Table 1). These data indicate that domestic pigs fed with high fat/fructose diets display some characteristics of human metabolic syndrome.

Adaption of adipose tissue in obesity

As showed in Figure 2, both subcutaneous (A) and pericardial (B) adipose tissue accumulations were greater in obese than in lean pigs. In subcutaneous abdominal adipose tissue, adipocyte size gradually increased in obese pigs, and at 12 and 16 weeks was significantly elevated compared to lean pigs (Figure 2C). Contrarily, at 16 wks there was no

significant difference between obese and lean pigs in the size of pericardial adipocytes (p=0.1, Figure 2D). Subcutaneous adipose tissue also showed increased capillary density and fibrosis, which were not observed in the pericardial adipose tissue (Figure 2E).

In subcutaneous adipose tissue, CD68/iNOS double-positive M1-macrophages were significantly and similarly increased in obese pigs from 8 weeks to 16 weeks, while the number of CD68/arginase-1 double-positive M2-macrophages increased only in obese pigs at 16 compared with 8 weeks and compared with lean (Figure 3A). In pericardial adipose tissue, only the number of M1 macrophages was significantly increased in obese compared with lean pigs (Figure 3B). Interestingly, real-time RT-PCR showed that mRNAs of M1 (CD86, CD11c), M2 (Arginase-1, mannose receptor), and macrophage (CD-68) markers were 2-fold increased compared to lean only in pericardial adipose tissue, while TNF-α mRNA increased in both subcutaneous and pericardial fat (Figure 3C and D). Immunohistochemistry also showed that TNF-α and IL-6 expression increased progressively and by 12 weeks became significant in subcutaneous abdominal fat of obese pigs (Figure 4A-B), but not in their pericardial fat (Figure 4C-D), suggesting a dissociation between macrophage phenotype and inflammatory markers in adipose tissue. Both subcutaneous and pericardial adipose tissue in obese showed a significant increase in MCP-1 expression at 16 weeks compared to Lean pigs (Figure 5A-B).

Cardiac hemodynamics and function

At 16 weeks, obese pigs had increased heart rate and rate pressure product (Table 1). Cardiac systolic (stroke volume, cardiac output, and ejection fraction) and diastolic (E/A ratio, p=0.3) function was similar in both groups (Table 1). Basal CT-derived myocardial perfusion was slightly but significantly lower in obese (Table 1, p=0.003), yet increased in response to adenosine in both lean and obese pigs (Table 1). Notably, both circulating and subcutaneous levels of MCP-1 inversely correlated with myocardial perfusion, but this correlation was not observed for pericardial MCP-1 (Figure 5C-E).

Furthermore, basal myocardial R_2* values were elevated in obese compared with lean pigs, suggesting myocardial hypoxia, but in neither group did they fall in response to adenosine (Figure 5F).

Discussion

This study shows that domestic pigs fed with a high-carbohydrate and -fat diet develop abdominal obesity, hypertension, high triglycerides, and insulin resistance, which constitute the most common features of human metabolic syndrome. We observed both morphological and biological remodeling of the adipose tissue during the development of obesity in this novel porcine model, including increases in adipocyte size and both abdominal subcutaneous and pericardial adipose tissue volume in obese pigs. An increase in M1-macrophage markers was observed in both subcutaneous and pericardial fat, as was elevation in both systemic levels and fat tissue expression of the inflammatory cytokine TNF-alpha and chemokine MCP-1. Inflammatory factors derived from the abdominal and pericardial depots may contribute to the increased circulating inflammatory cytokine levels in obese, which may impair myocardial perfusion, as we observed in vivo.

Conceptually, the subcutaneous fat belongs to systemically-acting fat depots, which include visceral, hepatic, muscle, or neck fat[28]. Locally-acting fat depots include pericardial, perivascular, and renal sinus fat. Previous studies show that accumulation of abdominal visceral fat, compared with overall obesity, has an equally or more important role in the development of cardiometabolic risk[29]. Locally-acting fat depots affect primarily adjacent anatomic organs, directly via lipotoxicity and indirectly via cytokine secretion. A previous study[30] implicated pericardial fat with coronary atherosclerosis, and our results suggest that both systemically-and locally-acting fat depots contribute to impaired cardiac function.

An important limitation to the study of the pathogenesis of metabolic disorders is the lack of large animal models with which to rigorously investigate the progression and biological mechanisms of the disease processes. Rodent models are useful[31, 32], small, and inexpensive, but exhibit important metabolic differences from primates, particularly in lipoprotein metabolism, the major site of lipogenesis (liver vs. fat), and in adipose tissue characteristics[33]. Monkeys are relatively large in size, exhibit great similarity to human physiology, and develop insulin resistance, dyslipidemia, hypertension, and type II diabetes with adult-onset metabolic syndrome[34]. However, potential spread of disease and ethical concerns limit the use of non-human primates in research. Importantly, pigs show many genetic, anatomical and physiological similarities to humans, allow using clinically-applicable medical tools and interventions, and provide ample blood and tissue samples for ex-vivo analysis. The Ossabaw mini-pig strain[26, 27] is a particularly valuable model, which when fed a high-fat/fructose diet develops many aspects of the obese, thanks to its thrifty phenotype. However, their availability is somewhat limited compared to domestic pigs and their body size smaller than humans'.

Domestic farm pigs offer the advantages of large body size, genetic diversity, and low cost. However, we have previously found that domestic pigs fed with high-fat/high-calorie diet were characterized by dyslipidemia and vascular dysfunction (e.g., reduced coronary endothelium-dependent vasorelaxation), but little abdominal obesity, spontaneous hypertension, or insulin resistance[12]. In the current study we found that feeding domestic pigs with a diet containing high levels of fructose, fat, and cholesterol over 16wks induced abdominal obesity, hypertension, high LDL and triglycerides, and insulin resistance, common features of human obese. Previous studies have shown that a high fat and fructose diet can induce insulin resistance in rats[13, 14], Ossabaw mini-pigs[15, 16], and Yucatan micropigs[35]. This diet may induce multiple abnormalities of insulin signaling by diminishing the association of PI3-kinase with insulin receptor substrate (IRS)-1 in response to insulin and increased serine-307 phosphorylation of IRS-1[35]. Interestingly, although still higher in obese than in lean, plasma triglyceride levels in both groups fell at 16 compared with their 12 weeks levels. This may possibly be related to the fact that when young animal approach adulthood, they tend to use more lipid fuel. Anage-related decrease in circulating lipids was also observed in a murine obese model[36].

Insulin resistance and visceral obesity have been recognized as important pathogenic factors in obesity. Subcutaneous fat represents a metabolically active organ, strongly related to insulin sensitivity. Mediating the secretion of adipocytokines like adiponectin, TNF-α, IL-6 and resistin, it is associated with the processes of inflammation, endothelial dysfunction,

hypertension and atherogenesis. Accordingly, in our domestic pig obese model, the circulating levels of adiponectin, which is considered a protective adipokine, declined at 16 compared to 12 weeks (although not compared to lean pigs). MCP-1 expression was elevated in subcutaneous adipose tissue, accompanied by inflammatory polarization in macrophages phenotype. These activated macrophages may secrete inflammatory cytokines, such as TNF-α and IL-6 that we observed to gradually increase in obese subcutaneous adipose tissue, reflecting metabolic activation of the adipose tissue as an endocrine organ. While plasma IL-6 levels and fat mRNA expression were not increased in our model (suggesting that IL-6 was not produced in-situ), elevated systemic TNF-α level may have contributed to insulin resistance and impaired myocardial perfusion. TNF-α induces not only vascular endothelial dysfunction[37], but also vascular remodeling[38]. We have previously shown that development of insulin resistance and obesity was characterized by myocardial hypoxia[5]. The decreased myocardial oxygenation detected by BOLD–MRI in obese might be secondary to an impairment in not only myocardial perfusion, but also glucose utilization[5], because macrophages and cytokines detected in obese may blunt myocardial glucose metabolism[39]. This link to inflammation was further supported by an inverse correlation between circulating as well as subcutaneous MCP-1 and myocardial perfusion in the current study.

We observed enhanced capillary density in subcutaneous adipose tissue, which may be a compensatory response to support marked adipose volume expansion. Local inflammation may be the major cause for the pathological remodeling of the subcutaneous adipose tissue. Pericardial fat has been implicated in the pathogenesis of coronary atherosclerosis[40], and is associated with elevated TNF-α levels[30]. We found that pericardial fat volume increased in our obese pig, as did visceral fat volume, and ex-vivo studies revealed that while MCP-1 expression and TNF-α mRNA were upregulated in pericardial fat, as were markers of M1 macrophages. These observations imply that inflammation and remodeling proceed in both abdominal subcutaneous and pericardial fat. Thus, increased systemic TNF-α level in our obese pig may have resulted from enhanced inflammation of abdominal and pericardial fat tissues.

Limitations

The study is limited by use of relatively young animals and short diet duration, yet this model recapitulates many features of obesity in humans. Alas, their large size may present difficulty in handling in long-term interventional studies, such as those needed to document development of cardiac dysfunction. Longitudinal biopsies of pericardial fat were not available. The reason for the apparent discrepancy between immunofluorescence and PCR in macrophage markers may be that only double-positive cells are counted as macrophages (e.g., CD68+/iNOS+ or CD68+/arginase-1+), whereas PCR measures single markers. Indeed, both methods revealed adipose inflammation, an important component of obesity. Further studies will need to explore the physiological pathways affecting the adipose tissue and its implications.

In summary, we evaluated a novel domestic porcine model of obesity, which shows many similarities to human disease, including adipose tissue remodeling and pro-inflammatory shift. This model provides a useful tool for research in metabolic diseases.

Acknowledgments

This study was partly supported by NIH grants: DK73608, HL121561, U01DK104273, C06-RR018898, UL1-TR000135, and the Mayo Clinic Center for Regenerative Medicine.

References

1. Eckel RH. Obeseesity and heart disease: A statement for healthcare professionals from the nutrition committee, american heart association. Circulation. 1997; 96:3248–3250. [PubMed: 9386201]
2. Ford ES, Giles WH, Dietz WH. Prevalence of the obeseesity among us adults: Findings from the third national health and nutrition examination survey. JAMA. 2002; 287:356–359. [PubMed: 11790215]
3. Smith SR, Lovejoy JC, Greenway F, Ryan D, deJonge L, de la Bretonne J, Volafova J, Bray GA. Contributions of total body fat, abdominal subcutaneous adipose tissue compartments, and visceral adipose tissue to the metabolic complications of obeseesity. Metabolism. 2001; 50:425–435. [PubMed: 11288037]
4. Cheng KH, Chu CS, Lee KT, Lin TH, Hsieh CC, Chiu CC, Voon WC, Sheu SH, Lai WT. Adipocytokines and proinflammatory mediators from abdominal and epicardial adipose tissue in patients with coronary artery disease. Int J Obesees (Lond). 2008; 32:268–274.
5. Li ZL, Woollard JR, Ebrahimi B, Crane JA, Jordan KL, Lerman A, Wang SM, Lerman LO. Transition from obeseesity to obeseesity is associated with altered myocardial autophagy and apoptosis. Arterioscler Thromb Vasc Biol. 2012; 32:1132–1141. [PubMed: 22383702]
6. Nishimura S, Manabe I, Nagai R. Adipose tissue inflammation in obeseesity and obeseesity. Discov Med. 2009; 8:55–60. [PubMed: 19788868]
7. Wisse BE. The inflammatory syndrome: The role of adipose tissue cytokines in metabolic disorders linked to obeseesity. J Am Soc Nephrol. 2004; 15:2792–2800. [PubMed: 15504932]
8. Malavazos AE, Ermetici F, Coman C, Corsi MM, Morricone L, Ambrosi B. Influence of epicardial adipose tissue and adipocytokine levels on cardiac abnormalities in visceral obeseesity. Int J Cardiol. 2007; 121:132–134. [PubMed: 17107724]
9. Mazurek T, Zhang L, Zalewski A, Mannion JD, Diehl JT, Arafat H, Sarov-Blat L, O'Brien S, Keiper EA, Johnson AG, Martin J, Goldstein BJ, Shi Y. Human epicardial adipose tissue is a source of inflammatory mediators. Circulation. 2003; 108:2460–2466. [PubMed: 14581396]
10. Zhang X, Li ZL, Woollard JR, Eirin A, Ebrahimi B, Crane JA, Zhu XY, Pawar AS, Krier JD, Jordan KL, Tang H, Textor SC, Lerman A, Lerman LO. Obeseesity-metabolic derangement preserves hemodynamics but promotes intrarenal adiposity and macrophage infiltration in swine renovascular disease. Am J Physiol Renal Physiol. 2013; 305:F265–276. [PubMed: 23657852]
11. Chade AR, Lerman A, Lerman LO. Kidney in early atherosclerosis. Hypertension. 2005; 45:1042–1049. [PubMed: 15897370]
12. Galili O, Versari D, Sattler KJ, Olson ML, Mannheim D, McConnell JP, Chade AR, Lerman LO, Lerman A. Early experimental obeseesity is associated with coronary endothelial dysfunction and oxidative stress. Am J Physiol Heart Circ Physiol. 2007; 292:H904–911. [PubMed: 17012356]
13. Kawamura T, Yoshida K, Sugawara A, Nagasaka M, Mori N, Takeuchi K, Kohzuki M. Impact of exercise and angiotensin converting enzyme inhibition on tumor necrosis factor-alpha and leptin in fructose-fed hypertensive rats. Hypertens Res. 2002; 25:919–926. [PubMed: 12484517]
14. Togashi N, Ura N, Higashiura K, Murakami H, Shimamoto K. The contribution of skeletal muscle tumor necrosis factor-alpha to insulin resistance and hypertension in fructose-fed rats. J Hypertens. 2000; 18:1605–1610. [PubMed: 11081773]

15. Clark BA, Alloosh M, Wenzel JW, Sturek M, Kostrominova TY. Effect of diet-induced obeseesity and obeseesity on skeletal muscles of ossabaw miniature swine. Am J Physiol Endocrinol Metab. 2011; 300:E848–857. [PubMed: 21304063]
16. Lee L, Alloosh M, Saxena R, Van Alstine W, Watkins BA, Klaunig JE, Sturek M, Chalasani N. Nutritional model of steatohepatitis and obeseesity in the ossabaw miniature swine. Hepatology. 2009; 50:56–67. [PubMed: 19434740]
17. Zhu XY, Daghini E, Chade AR, Napoli C, Ritman EL, Lerman A, Lerman LO. Simvastatin prevents coronary microvascular remodeling in renovascular hypertensive pigs. JAm Soc Nephrol. 2007; 18:1209–1217. [PubMed: 17344424]
18. Warner L, Glockner JF, Woollard J, Textor SC, Romero JC, Lerman LO. Determinations of renal cortical and medullary oxygenation using blood oxygen level-dependent magnetic resonance imaging and selective diuretics. Invest Radiol. 2011; 46:41–47. [PubMed: 20856128]
19. Li Z, Woollard JR, Wang S, Korsmo MJ, Ebrahimi B, Grande JP, Textor SC, Lerman A, Lerman LO. Increased glomerular filtration rate in early obeseesity is associated with renal adiposity and microvascular proliferation. Am J Physiol Renal Physiol. 2011; 301:F1078–1087. [PubMed: 21775485]
20. Ebrahimi B, Gloviczki M, Woollard JR, Crane JA, Textor SC, Lerman LO. Compartmental analysis of renal bold mri data: Introduction and validation. Invest Radiol. 2012; 47:175–182. [PubMed: 22183077]
21. Ebrahimi B, Eirin A, Li Z, Zhu XY, Zhang X, Lerman A, Textor SC, Lerman LO. Mesenchymal stem cells improve medullary inflammation and fibrosis after revascularization of swine atherosclerotic renal artery stenosis. PLoS One. 2013; 8:e67474. [PubMed: 23844014]
22. Warner L, Yin M, Glaser KJ, Woollard JA, Carrascal CA, Korsmo MJ, Crane JA, Ehman RL, Lerman LO. Noninvasive in vivo assessment of renal tissue elasticity during graded renal ischemia using mr elastography. Invest Radiol. 2011; 46:509–514. [PubMed: 21467945]
23. Urbieta-Caceres VH, Lavi R, Zhu XY, Crane JA, Textor SC, Lerman A, Lerman LO. Early atherosclerosis aggravates the effect of renal artery stenosis on the swine kidney. Am J Physiol Renal Physiol. 2010; 299:F135–140. [PubMed: 20462971]
24. Zhu XY, Daghini E, Chade AR, Versari D, Krier JD, Textor KB, Lerman A, Lerman LO. Myocardial microvascular function during acute coronary artery stenosis: Effect of hypertension and hypercholesterolaemia. Cardiovasc Res. 2009; 83:371–380. [PubMed: 19423617]
25. Zhu XY, Daghini E, Chade AR, Rodriguez-Porcel M, Napoli C, Lerman A, Lerman LO. Role of oxidative stress in remodeling of the myocardial microcirculation in hypertension. Arterioscler Thromb Vasc Biol. 2006; 26:1746–1752. [PubMed: 16709946]
26. Daghini E, Primak AN, Chade AR, Zhu X, Ritman EL, McCollough CH, Lerman LO. Evaluation of porcine myocardial microvascular permeability and fractional vascular volume using 64-slice helical computed tomography (ct). Invest Radiol. 2007; 42:274–282. [PubMed: 17414522]
27. Li ZL, Ebrahimi B, Zhang X, Eirin A, Woollard JR, Tang H, Lerman A, Wang S, Lerman LO. Obeseesity-metabolic derangement exacerbates cardiomyocyte loss distal to moderate coronary artery stenosis in pigs without affecting globeseal cardiac function. Am J Physiol Heart Circ Physiol. 2014
28. Lim S, Meigs JB. Ectopic fat and cardiometabolic and vascular risk. Int J Cardiol. 2013
29. Lim S, Meigs JB. Ectopic fat and cardiometabolic and vascular risk. Int J Cardiol. 2013; 169:166–176. [PubMed: 24063931]
30. Greif M, Becker A, von Ziegler F, Lebherz C, Lehrke M, Broedl UC, Tittus J, Parhofer K, Becker C, Reiser M, Knez A, Leber AW. Pericardial adipose tissue determined by dual source ct is a risk factor for coronary atherosclerosis. Arterioscler Thromb Vasc Biol. 2009; 29:781–786. [PubMed: 19229071]
31. Scott NJ, Cameron VA, Raudsepp S, Lewis LK, Simpson ER, Richards AM, Ellmers LJ. Generation and characterization of a mouse model of the obeseesity: Apolipoprotein e and aromatase double knockout mice. Am J Physiol Endocrinol Metab. 2012; 302:E576–584. [PubMed: 22185842]
32. Fukuda D, Aikawa E, Swirski FK, Novobeserantseva TI, Kotelianski V, Gorgun CZ, Chudnovskiy A, Yamazaki H, Croce K, Weissleder R, Aster JC, Hotamisligil GS, Yagita H, Aikawa M. Notch

ligand delta-like 4 blockade attenuates atherosclerosis and metabolic disorders. Proc Natl Acad Sci U S A. 2012; 109:E1868–1877. [PubMed: 22699504]

33. Arner P. Resistin: Yet another adipokine tells us that men are not mice. Diabetologia. 2005; 48:2203–2205. [PubMed: 16193286]
34. Bremer AA, Stanhope KL, Graham JL, Cummings BP, Wang W, Saville BR, Havel PJ. Fructose-fed rhesus monkeys: A nonhuman primate model of insulin resistance, obeseesity, and type 2 diabetes. Clin Transl Sci. 2011; 4:243–252. [PubMed: 21884510]
35. Lee J, Xu Y, Lu L, Bergman B, Leitner JW, Greyson C, Draznin B, Schwartz GG. Multiple abnormalities of myocardial insulin signaling in a porcine model of diet-induced obeseesity. Am J Physiol Heart Circ Physiol. 2010; 298:H310–319. [PubMed: 19897715]
36. Menahan LA. Age-related changes in lipid and carbohydrate metabolism of the genetically obeseese mouse. Metabolism. 1983; 32:172–178. [PubMed: 6338347]
37. Donato AJ, Henson GD, Morgan RG, Enz RA, Walker AE, Lesniewski LA. Tnf-alpha impairs endothelial function in adipose tissue resistance arteries of mice with diet-induced obeseesity. Am J Physiol Heart Circ Physiol. 2012; 303:H672–679. [PubMed: 22821989]
38. Moe KT, Naylynn TM, Yin NO, Khairunnisa K, Allen JC, Wong MC, Chin-Dusting J, Wong P. Tumor necrosis factor-alpha induces aortic intima-media thickening via perivascular adipose tissue inflammation. J Vasc Res. 2013; 50:228–237. [PubMed: 23711955]
39. Ko HJ, Zhang Z, Jung DY, Jun JY, Ma Z, Jones KE, Chan SY, Kim JK. Nutrient stress activates inflammation and reduces glucose metabolism by suppressing amp-activated protein kinase in the heart. Diabetes. 2009; 58:2536–2546. [PubMed: 19690060]
40. Tadros TM, Massaro JM, Rosito GA, Hoffmann U, Vasan RS, Larson MG, Keaney JF Jr, Lipinska I, Meigs JB, Kathiresan S, O'Donnell CJ, Fox CS, Benjamin EJ. Pericardial fat volume correlates with inflammatory markers: The framingham heart study. Obeseesity (Silver Spring). 2010; 18:1039–1045.

What is already known about this subject

- Adipose tissue secrets adipokines and pro-inflammatory cytokines contribute to insulin resistance in obesity.
- Pre-clinical animal models of obesity with insulin resistance are limited.

What this study adds

- Domestic pigs fed with a high-carbohydrate and -fat diet develop obesity with insulin resistance.
- Adipose tissue-released inflammatory cytokines may impair myocardial perfusion.

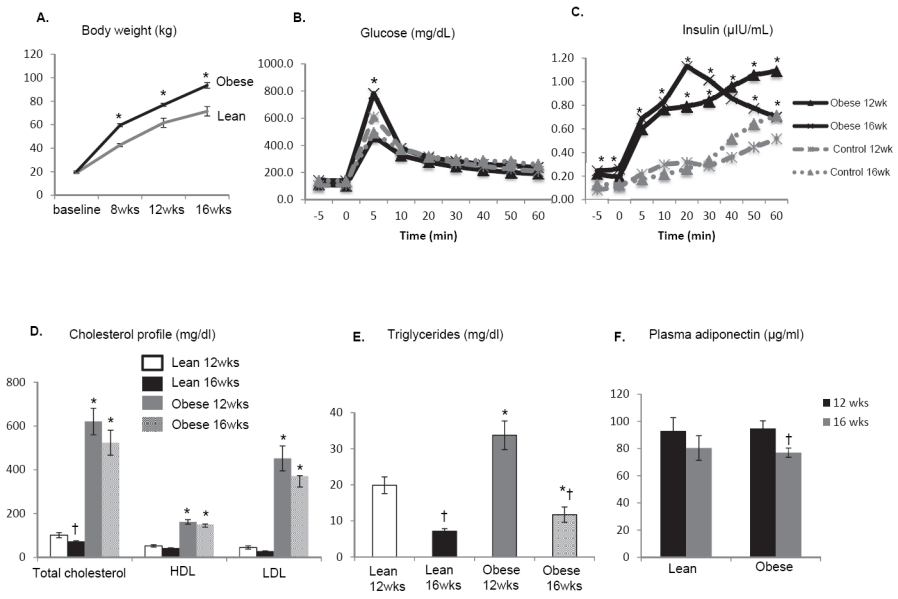

Figure 1.

Obese pigs progressively gained body weight more than lean (A). Plasma insulin levels increased during IVGTT in obese compared to lean pigs at 12 and 16 weeks (B-C). In obese pigs, total cholesterol, LDL, HDL, and serum triglycerides were elevated at 12 and 16 weeks. In lean pigs, both total cholesterol and triglycerides fell at 16 compared with 12 weeks, while in obese only triglycerides fell, but remained higher than in lean pigs (D-E). Plasma adiponectin levels were similar between lean and obese pigs, but were decreased only in obese pigs at 16 compared with 12 weeks (F). *p<0.05 vs. lean. †p<0.05 vs. 12wks

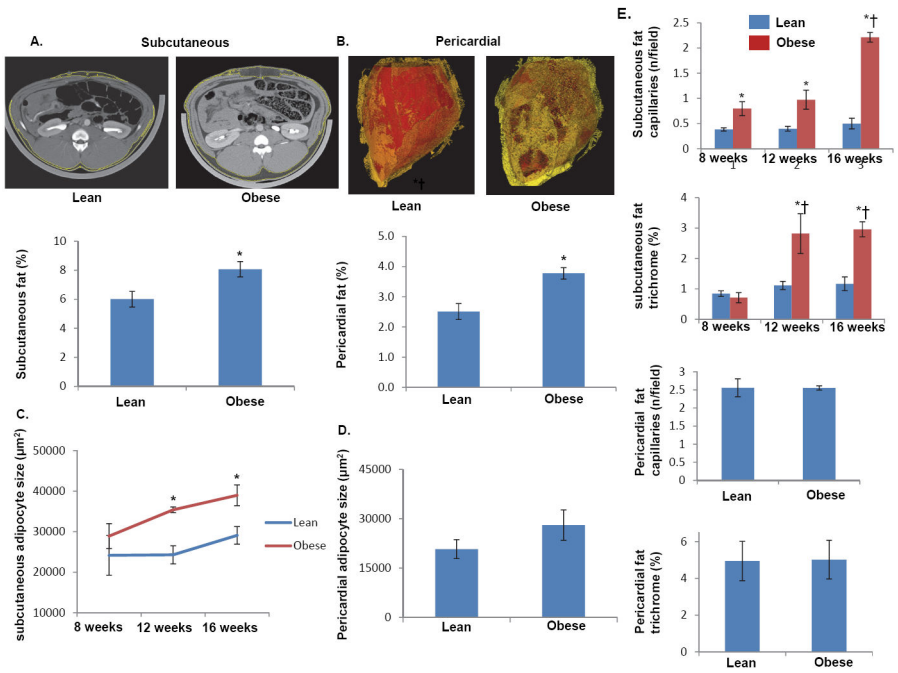

Figure 2.

Representative MDCT images of increased subcutaneous (A) and pericardial (B) adipose tissue and quantifications of their fractions. The size of subcutaneous and pericardial adipocytes during the development of obesity (C-D). Capillary count and trichrome analysis showing increased capillary density and adipose tissue fibrosis observed in abdominal adipose tissue (E). *p<0.05 vs. lean. †p<0.05 vs. 12wks

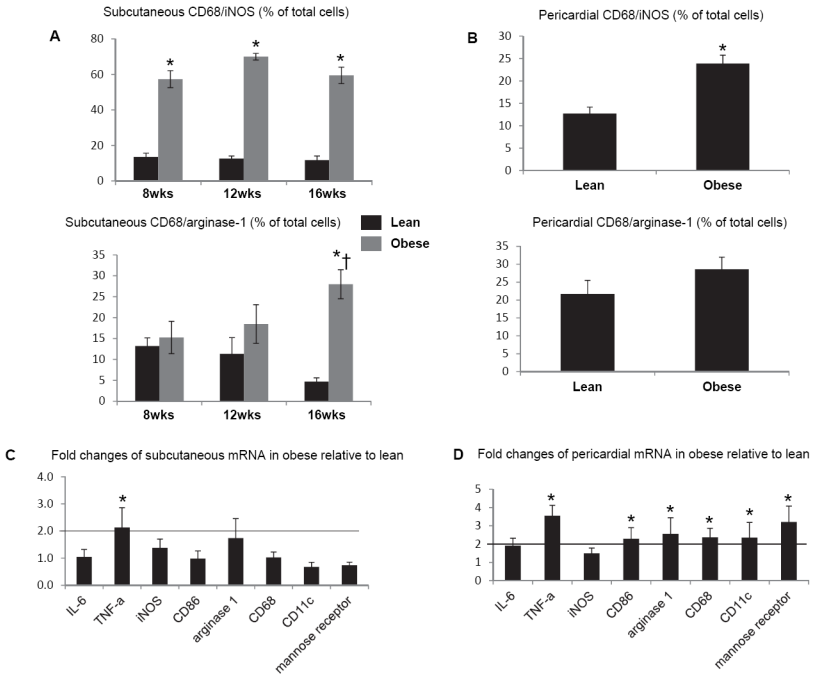

Figure 3.

In subcutaneous adipose tissue, the number of M1 macrophages similarly increased in obese pigs from 8 to 16 weeks, while the number of M2 macrophages only increased in obese pigs at 16 weeks compared with 8 weeks and with lean (A). In pericardial adipose tissue, only M1 macrophages increased in obese compared with lean (B). Macrophage mRNA (CD68) and both M1 (CD 86, CD11c) and M2 (Arginase-1, mannose-receptor) markers increased only in pericardial adipose tissue, while TNF-α mRNA increased in both subcutaneous and pericardial fat (C-D). *p<0.05 vs. lean. †p<0.05 vs. 12wks

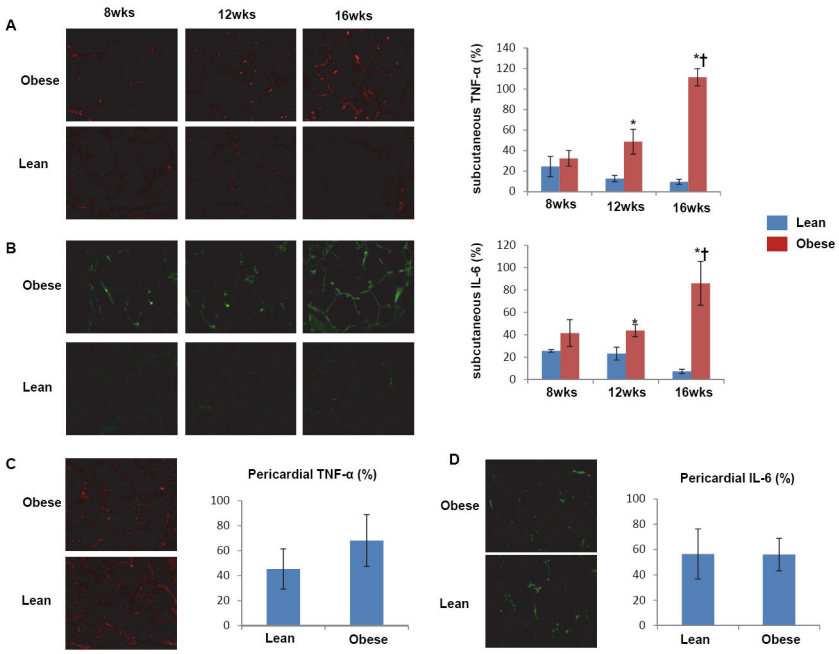

Figure 4.

Longitudinal changes in immunoreactivity of tumor necrosis-factor (TNF)-α and interleukin (IL)-6, showing upregulation of both at 12 and 16 weeks of swine obesity in abdominal (A&B) but not pericardial (C&D) fat tissue. *p<0.05 vs. lean. †p<0.05 vs. 12 wks.

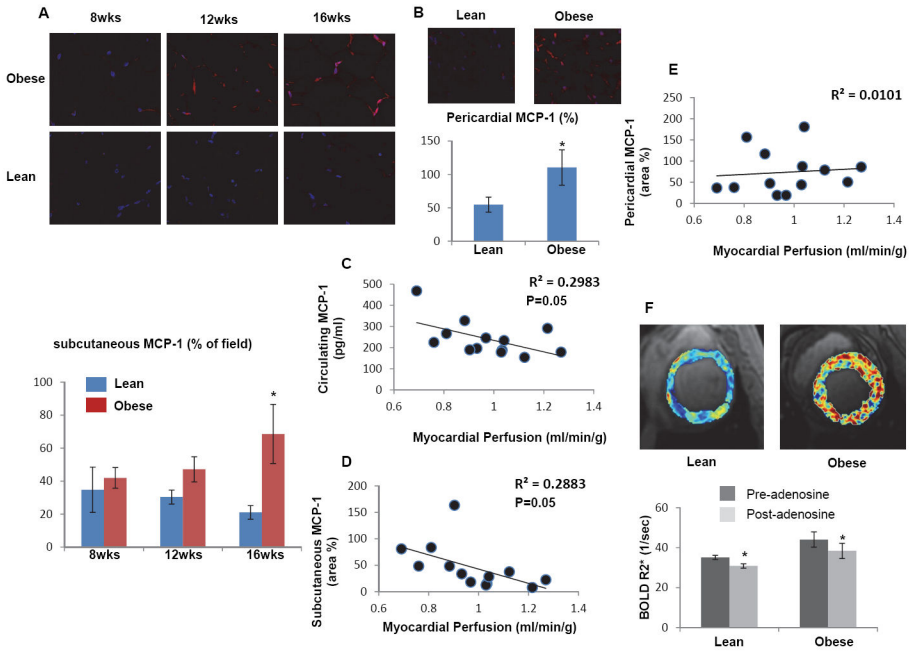

Figure 5.

Longitudinal changes in MCP-1 expression in subcutaneous (A) and pericardial (B) adipose tissue of obese pigs. Both circulating and subcutaneous MCP-1 inversely correlated with myocardial perfusion, but this correlation was not observed for pericardial MCP-1 (C-E). (F) Representative BOLD-MRI images showed increased myocardial hypoxia in obese pigs and quantification of R2*. *p<0.05 vs. lean.

Table 1

Systemic and cardiac functional measurements (mean±SEM) in domestic pigs after 16 weeks of lean or obese diet.

	Lean (n=7)	Obese (n=7)
Body weight (kg)	71.4±4	93.4±0.9*
Mean arterial pressure (mmHg)	102.7±3.6	124.2±4*
Creatinine (mg/dl)	1.3±0.2	1.3±0.1
HOMA-IR score	0.7±0.07	1.8±0.4*
Monocyte chemoattractant protein-1 (pg/ml)	204.2±17.9	312.9±31.6*
Tumor necrosis factor-1 (pg/ml)	70.1±7.6	208.2±62.7*
Heart rate (beats/minute)	71.9±2.8	86.0±5.8*
Rate pressure product	9100.4±483.5	12186.0±862.2*
Stroke volume (ml)	72.46±4.12	71.82±4.26
Cardiac output (L)	5.2±0.4	6.1±0.3
Ejection fraction (%)	54.69±1.37	52.35±2.80
E/A	1.06±0.1	0.9±0.1
Myocardial perfusion (ml/min/g)		
Baseline	1.08±0.04	0.84±0.3*
Adenosine	1.34±0.12+	1.05±0.4*+
Change after adenosine (%)	23.7±8.2	27.6±11.8

*p<0.05 vs. lean,

+p<0.05 vs. baseline.

HOMA-IR: homeostasis model assessment of insulin resistance.